The structure of the high-energy spin excitations in a high-transition-temperature superconductor

S. M. Hayden[1], H. A. Mook[2], Pengcheng Dai[2,3], T. G. Perring[4] & F. Doğan[5]

[1]H. H. Wills Physics Laboratory, University of Bristol, Bristol BS8 1TL, UK
[2]Condensed Matter Sciences Division, Oak Ridge National Laboratory, Oak Ridge, Tennessee 37831-6393, USA
[3]Department of Physics and Astronomy, The University of Tennessee, Knoxville, Tennessee 37996-1200, USA
[4]ISIS Facility, Rutherford Appleton Laboratory, Chilton, Oxon OX11 0QX, UK
[5]Department of Ceramic Engineering, University of Missouri-Rolla, Rolla, Missouri 65409-0330, USA

In conventional superconductors, lattice vibrations (phonons) mediate the attraction between electrons that is responsible for superconductivity[1]. The high transition temperatures (high-T_c) of the copper oxide superconductors has led to collective spin excitations being proposed as the mediating excitations in these materials[2]. The mediating excitations must be strongly coupled to the conduction electrons, have energy greater than the pairing energy, and be present at T_c. The most obvious feature in the magnetic excitations of high-T_c superconductors such as $YBa_2Cu_3O_{6+x}$ is the so-called 'resonance'[3–6]. Although the resonance may be strongly coupled to the superconductivity[3–8], it is unlikely to be the main cause, because it has not been found in the $La_{2-x}(Ba,Sr)_xCuO_4$ family and is not universally present in $Bi_2Sr_2CaCu_2O_{8+\delta}$ (ref. 9). Here we use inelastic neutron scattering to characterize possible mediating excitations at higher energies in $YBa_2Cu_3O_{6.6}$. We observe a square-shaped continuum of excitations peaked at incommensurate positions. These excitations have energies greater than the superconducting pairing energy, are present at T_c, and have spectral weight far exceeding that of the 'resonance'. The discovery of similar excitations in $La_{2-x}Ba_xCuO_4$ (ref. 10) suggests that they are a general property of the copper oxides, and a candidate for mediating the electron pairing.

In a conventional superconductor, the modification of the phonons[11] on entering the superconducting state indicates the presence of strong electron–phonon coupling. The dramatic changes seen in the magnetic excitation spectrum[3–6,12–15] as copper oxide superconductors enter the superconducting state points to a strong coupling of the magnetic excitations and superconductivity. The magnetism in superconducting copper oxides arises from the incomplete outer shells of the copper ions and fluctuations in these unpaired spins give rise to collective magnetic excitations, which are coherent over many lattice sites. We use neutron scattering to probe the wavevector (**Q**) and energy (E) dependence of the spin fluctuations in $YBa_2Cu_3O_{6.6}$. To label the two-dimensional reciprocal space which corresponds to the CuO_2 planes, we use reciprocal lattice vectors such that (1,0) and (0,1) are along the lines joining nearest-neighbour copper atoms. In this notation, the magnetic excitations are strongest near the $\mathbf{Q} = (1/2,1/2)$ position. The most prominent feature of the magnetic excitations in the superconducting state of the $YBa_2Cu_3O_{6+x}$ system, where x controls the hole-doping level, is the 'resonance' (refs 3–6). The resonance occurs at (1/2,1/2) and at energies of 41 meV for optimally doped $YBa_2Cu_3O_{6.93}$, where T_c is at the highest value, and at 34 meV for underdoped $YBa_2Cu_3O_{6.6}$, where x and T_c are below their optimal values[3–6]. For energies below the resonance energy, E_{res}, the magnetic excitations are peaked away from (1/2,1/2) at the incommensurate positions $(1/2 \pm \delta,1/2)$ and $(1/2,1/2 \pm \delta)$, with $\delta = 0.105$ for $YBa_2Cu_3O_{6.6}$ (refs 12, 13).

Although the magnetic excitations associated with the 'resonance' are obviously important because they show dramatic enhancement below T_c, they contain only a small part of the total spectral weight[5,6]. Thus we need to understand the higher-energy excitations better because they may mediate electron pairing. Experimentally, magnetic excitations have been observed for energies above E_{res} in underdoped $YBa_2Cu_3O_{6+x}$ for energies up to about 120 meV (refs 5, 14, 16–18). Neutron-scattering measurements, performed using a three-axis spectrometer at a reactor[16,18], have shown that for energies greater than the resonance energy $E > E_{res}$, the magnetic response also peaks away from the (1/2,1/2) position. However, technical limitations have meant that the wavevector dependence of the high-energy excitations has not been determined. Here we use a time-of-flight neutron spectrometer equipped with position-sensitive detectors to measure the $E > E_{res}$ excitations in well-characterized $YBa_2Cu_3O_{6.6}$ with $T_c = 62.7$ K and $E_{res} = 34$ meV (refs 5, 12, 13, 17).

Figure 1a–c shows images of the magnetic scattering for the energy $E = 85$ meV at $T = 10$ K, 66 K ($T_c + 3.3$ K) and 300 K. At high temperatures (Fig. 1a) the magnetic response consists of a single peak centred on the (1/2,1/2) position. As the temperature is lowered through T_c, a quartet of peaks is formed at the positions $\mathbf{Q}_\epsilon = (1/2 \pm \epsilon, 1/2 \pm \epsilon)$ and $(1/2 \pm \varepsilon, 1/2 \mp \varepsilon)$, with $\epsilon = 0.12 \pm 0.01$ reciprocal lattice units (r.l.u.) (for $E = 85$ meV). The pattern is very different from the low-energy scattering observed in the same $YBa_2Cu_3O_{6.6}$ sample in that the four peaks at high-energy $E \approx 85$ meV are rotated by 45 degrees with respect to those observed at lower energy $E \approx 24$ meV (refs 12–15). The low-energy incommensurate peaks are shown in Fig. 2f. Figure 1d–f shows cuts along the diagonals of Fig. 1a–c. Coherent high-energy excitations peaked at (1/2,1/2) are present at $T = 300$ K, the incommensurate structure appears between 300 and 66 K and is almost fully developed by $T = 66\ \mathrm{K} = T_c + 3.3$ K. For comparison, Fig. 1g–i shows Q–E maps of the intensity of the low-energy magnetic excitations measured for $\mathbf{Q} = (1/2,k)$. The trajectory of this path passes through the low-energy incommensurate peaks at $(1/2,1/2 \pm \delta)$. As the temperature is lowered from 300 to 66 K ($T_c + 3.3$ K), the magnetic response becomes strong near (1/2,1/2) and $E_{res} = 34$ meV. Further lowering the temperature leads to the resonance becoming stronger and incommensurate peaks developing below E_{res}. In contrast, the high-energy incommensurate peaks are fully developed at T_c. Both the low-energy and the high-energy incommensurate peaks develop through a loss of spectral weight near (1/2,1/2) and at their respective energies as the temperature is lowered.

To obtain a more complete picture of the high-energy response we collected data at four energies above the resonance energy. The evolution of the magnetic response with energy is shown in Fig. 2a–f. For the lowest energy probed above the resonance, $E = 66$ meV, we observe a square structure with the vertices of the square pointing along the (110) and $(1\bar{1}0)$ directions. There is evidence that the response is strongest near the edge of the square: a cut along $(1/2-h,1/2+h)$ (see Fig. 2j) shows incommensurate peaks away from (1/2,1/2). The incommensurate peaks are most developed in the energy range 70–90 meV: Fig. 2b and c clearly shows four peaks. At the highest energy studied (Fig. 2a), $E = 105$ meV, the scattering still displays the square structure observed for $E = 66$ meV and is peaked away from (1/2,1/2). However, a four-peak structure is not discernible. Figure 2j–l shows cuts through the (1/2,1/2) position. The solid lines are fits to the phenomenological response function $\chi''(\mathbf{Q},\omega) = \sum_\varepsilon A\xi^4\left(\xi^2 + (\mathbf{Q}-\mathbf{Q}_\varepsilon)^2\right)^{-2}$, where the sum is over the incommensurate wavevectors $\mathbf{Q}_\epsilon$. It is interesting to compare the wavevector and energy-integrated spectral weights of the high-energy response studied here with the resonance and low-energy incommensurate structure. We find $\langle m^2 \rangle = 0.12 \pm 0.02\mu_B^2$ per formula unit (f.u.) for the resonance and sub-resonance structure ($24 < E < 44$ meV) and $\langle m^2 \rangle = 0.26 \pm 0.05\mu_B^2\,\mathrm{f.u.}^{-1}$ for the high-energy scattering pictured in Fig. 2a–d ($60 < E < 120$ meV). Thus the higher-energy response has a significantly greater contribution to the total fluctuating moment than the resonance structure.

The present data show how structure develops in the high-energy magnetic excitation spectrum of an underdoped high-T_c copper oxide superconductor as it is cooled. The excitations develop their coherence between 300 and 66 K, that is, above the critical temperature T_c. Many other electronic properties, ranging from angle-resolved photoemission (ARPES)[19] to resistivity, show corresponding changes above T_c for underdoped compositions. Such behaviour is generally attributed to a higher temperature scale T^*—the temperature at which the pseudogap develops[20].

Our data show that the high-energy magnetic excitations in the high-temperature superconductor $YBa_2Cu_3O_{6.6}$ consists of a continuum of scattering bounded by a square and peaked at wavevector positions $(1/2 \pm \epsilon, 1/2 \pm \epsilon)$ and $(1/2 \pm \varepsilon, 1/2 \mp \varepsilon)$. A similar structure has recently been observed in the high-energy magnetic excitations of the magnetically ordered but weakly superconducting compound $La_{1.85}Ba_{0.125}CuO_4$ (ref. 10). This suggests there is universality, both in the low-energy[12–15,21] and the high-energy spin dynamics between two very different classes of high-T_c superconductor. The magnetism in the $YBa_2Cu_3O_{6+x}$ system derives from the antiferromagnetic parent compound $YBa_2Cu_3O_6$. Thus it has been widely assumed[22] that the high-energy dynamics are described by a short-range Heisenberg interaction with an exchange suitably reduced from the insulator value[23]. This leads to the high-energy excitations being spin-wave-like, such as in the

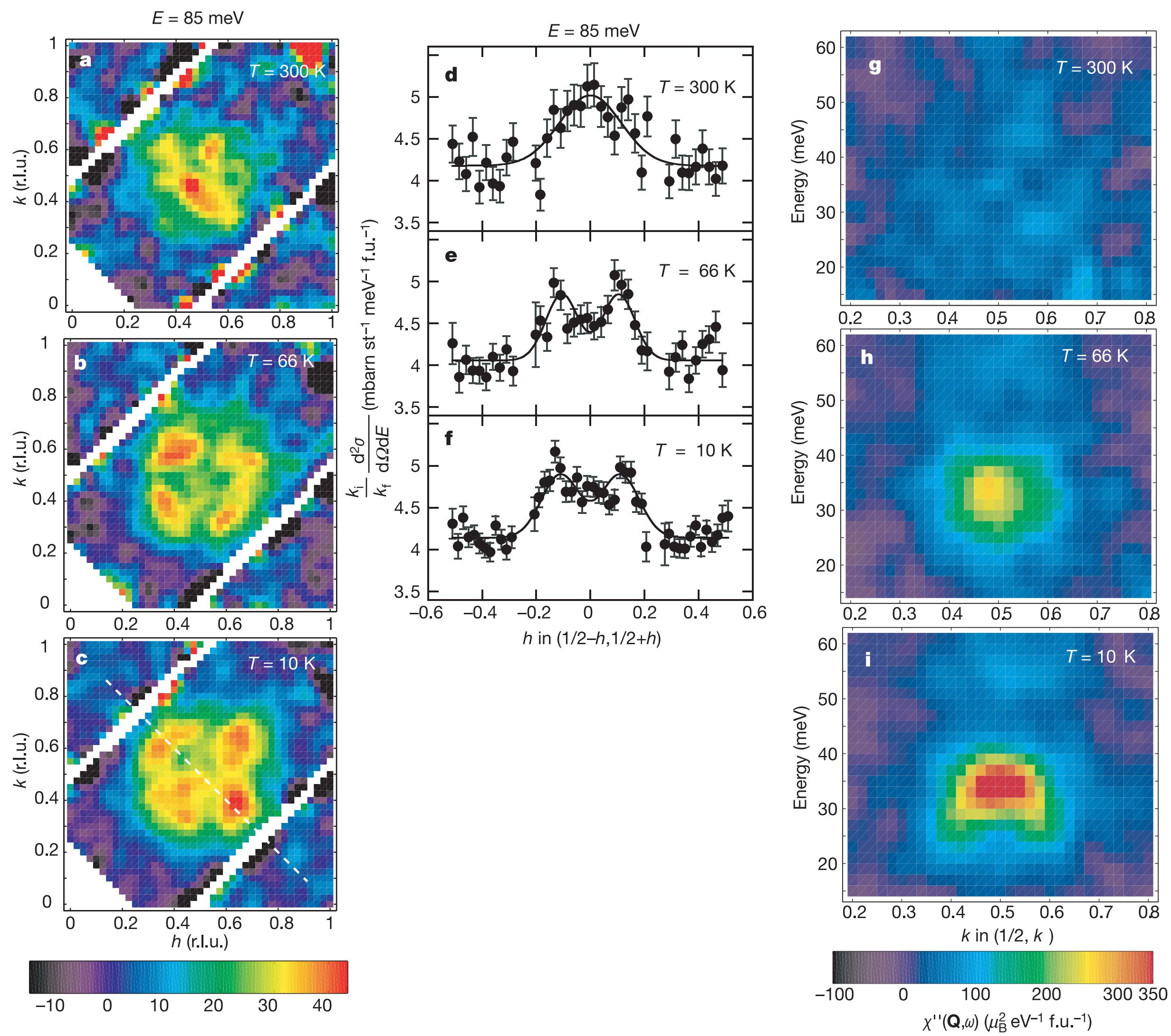

Figure 1 Images of the magnetic excitations in $YBa_2Cu_3O_{6.6}$, for various temperatures, measured by neutron scattering. **a**–**c**, Magnetic scattering at 300, 66 and 10 K showing the formation of the high-energy incommensurate peaks for $E = 85$ meV. **d**–**f**, Cuts through the incommensurate peaks along dashed line in **c** (no units conversion or background subtraction). A quadratic ($|\mathbf{Q}|^2$) background has been subtracted and data converted to absolute units. The bilayer structure of $YBa_2Cu_3O_{6.6}$ means that the magnetic excitations depend on the out-of-plane wavevector. The data shown here correspond to acoustic or odd excitations and were measured with $l = 5.4$ r.l.u., where $\mathbf{Q} = h\mathbf{a}^* + k\mathbf{b}^* + l\mathbf{c}^*$, $a^* = 2\pi/a$, in which $b^* = 2\pi/b$, $c^* = 2\pi/c$. The lattice parameters (in Å) are $a = 3.82$, $b = 3.88$, and $c = 11.743$ for $YBa_2Cu_3O_{6.6}$. **g**–**i**, The magnetic response $\chi''(\mathbf{Q},\omega)$ plotted as a function of wavevector and energy, for wavevectors along the dashed line in Fig. 2e. The data shown in **g**–**i** correspond to acoustic or odd excitations with $1.4 < l < 2.0$. A measured energy-dependent background determined in the region $0 < h < 0.25$ and $0.3 < k < 0.7$ has been subtracted from the data. Experiments were performed using the MAPS chopper spectrometer at the ISIS spallation neutron source. Data were measured with an incident neutron energy of 160 meV and have a counting time of 48 h with a source proton current of 170 μA. The 25-g single crystal sample was mounted in a thin-walled aluminium can. The MAPS spectrometer has an obstruction-free evacuated flight path to reduce background caused by air scattering. Data were generally collected at small scattering angles to minimize $|\mathbf{Q}|$, because the phonon and multiphonon scattering increases rapidly with $|\mathbf{Q}|$, while the magnetic scattering decreases with $|\mathbf{Q}|$. Data were placed on an absolute scale using a vanadium standard and corrected for the anisotropic Cu^{2+} $d_{x^2-y^2}$ form factor.

parent antiferromagnets above their Néel temperature. If such a picture were correct, our images (Fig. 2a–d) of the high-energy magnetic excitations should show rings of scattering (where the spin-wave dispersion intersects the corresponding constant-energy plane) that get bigger as the energy is increased. The instrumental resolution (see Fig. 2a–f) would be sufficient to resolve the ring structure (see Supplementary Information). In fact, there is relatively little dispersion in the data in the energy range

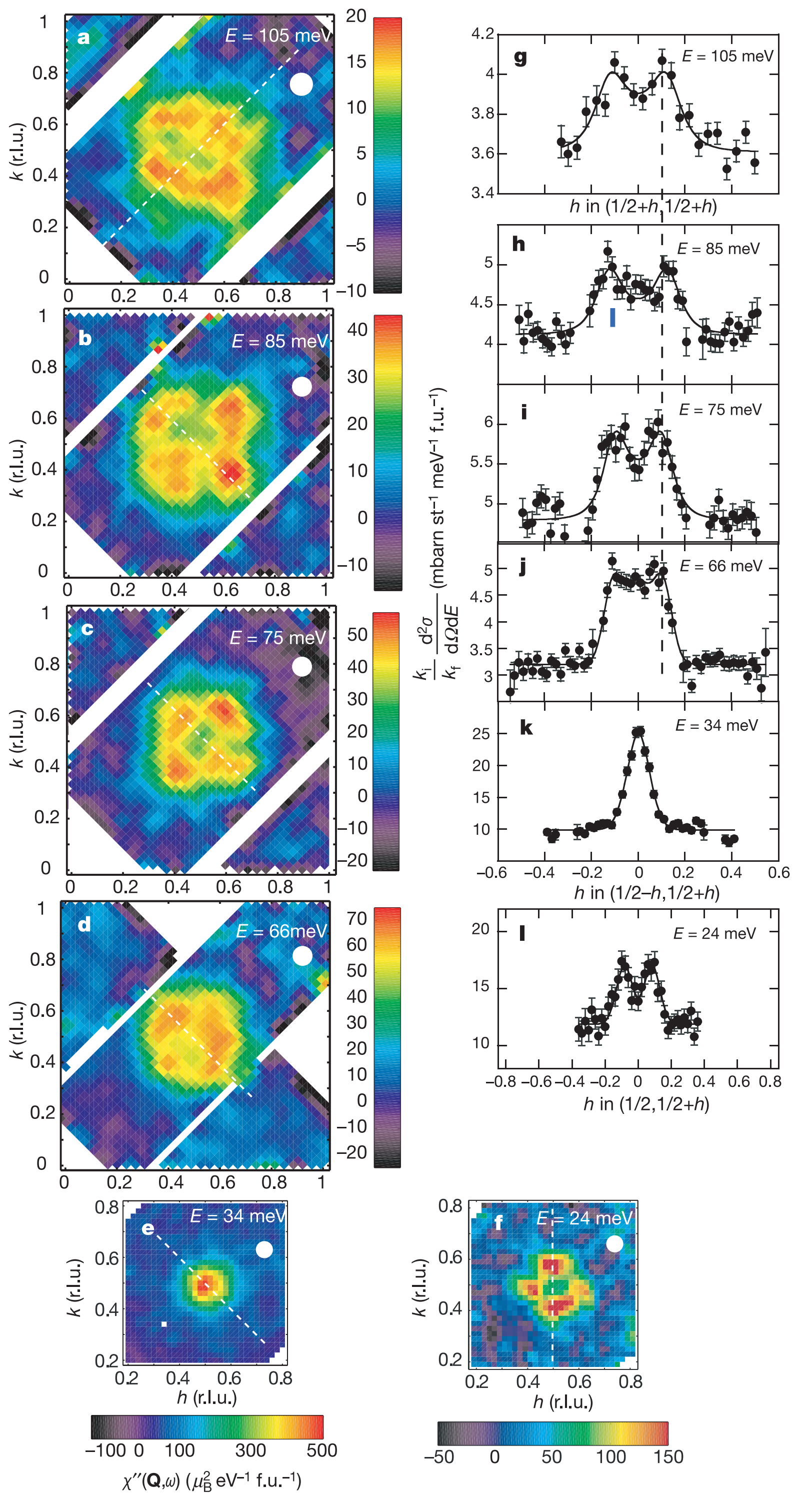

Figure 2 Images of the magnetic scattering in $YBa_2Cu_3O_{6.6}$ at $T = 10$ K for various excitation energies (frequencies). **a**–**f**, Magnetic excitations for energies between 24 and 105 meV. The data shown here correspond to acoustic or odd excitations and were measured with $l = 1.8$ or 5.4 r.l.u. **g**–**l**, Cuts through the (1/2,1/2) position along the dotted lines in **a**–**f**. The incident neutron energies used were 105, 160 and 220 meV. The $E = 105$ meV image was counted for 72 h. The white circles in **a**–**f** and the bar in **h** for $E = 85$ meV represent the approximate instrumental resolution. The ranges of integration for energy transfers $E = 24$, 34, 66, 75, 85 and 105 meV are $\Delta E = 6$, 6, 8, 10, 10 and 30 meV, respectively. The solid lines in **g**–**j** are fits to the equation given in the text, where $\epsilon = 0.09(1)$, 0.10(1), 0.12(1), 0.11(1) r.l.u. and $\xi = 0.09(1)$, 0.09(1), 0.10(1) and 0.10(2) r.l.u. for $E = 66$, 75, 85 and 105 meV respectively. The vertical dashed line through **g**–**j** is the average value of ϵ.

$66 < E < 105$ meV (see dashed line in Fig. 2g–j). Thus a spin-wave-like dispersion at high energies seems to be inconsistent with our data.

Given that the observed spin dynamics is qualitatively similar in the two classes of high-T_c superconductor where they have been studied, one might expect that they have a common underlying origin. Candidates for this common origin include an incipient spin-charge separation leading to unidirectional stripes[10,22] and the underlying electronic (band) structure. The high-energy magnetic excitations of stripes are strong along streaks in reciprocal space: these streaks can intersect to yield square-like structures. Alternatively, in an itinerant picture, the starting point for understanding the spin dynamics[24,25] are electron–hole pair excitations about an underlying Fermi surface[26]. This interpretation is supported by theoretical calculations performed using an itinerant approach based on a standard random phase approximation (RPA) that have predicted the correct geometry of the high-energy incommensurate peaks reported here[25].

The integrated spectral weight feature characterized here is considerably greater than the much sharper and widely discussed 'resonance' feature (Fig. 1j–i) present at lower energies[3–6]. The high-energy excitations reported here are also present at T_c. Thus, in a magnetically mediated pairing mechanism the high-energy structure would have the dominant contribution to the pairing interaction. One might expect mediating excitations in the superconducting copper oxides to be a property of the CuO_2 planes themselves, and so they should be similar in different systems. The observation[10] of high-energy magnetic excitations with a similar structure in $La_{1.875}Ba_{0.125}CuO_4$ supports this notion. □

Received 29 October 2003; accepted 16 April 2004; doi:10.1038/nature02576.

1. Bardeen, J., Cooper, L. N. & Schrieffer, J. R. Theory of superconductivity. *Phys. Rev.* **108,** 1175–1204 (1957).
2. Chubukov, A. V., Pines, D. & Schmalian, J. in *The Physics of Superconductors* Vol. I, *Conventional and High-T_c Superconductors* (eds Bennemann, K. H. & Ketterson, J. B.) 495–590 (Springer, Berlin, 2003).
3. Rossat-Mignod, J. *et al.* Neutron scattering study of the $YBa_2Cu_3O_{6+x}$ system. *Physica C* **185,** 86–92 (1991).
4. Mook, H. A., Yethiraj, M., Aeppli, G., Mason, T. E. & Armstrong, T. Polarized neutron determination of the magnetic excitations in $YBa_2Cu_3O_7$. *Phys. Rev. Lett.* **70,** 3490–3493 (1993).
5. Dai, P. *et al.* The magnetic excitation spectrum and thermodynamics of high-T_c superconductors. *Science* **284,** 1344–1347 (1999).
6. Stock, C. *et al.* Dynamic stripes and resonance in the superconducting and normal phases of $YBa_2Cu_3O_{6.5}$ ortho-II superconductor. *Phys. Rev. B* **69,** 014502 (2004).
7. Scalapino, D. J. & White, S. R. Superconducting condensation energy and an antiferromagnetic exchange-based pairing mechanism. *Phys. Rev. B* **58,** 8222–8224 (1998).
8. Demler, E. & Zhang, S. C. Quantitative test of a microscopic mechanism of high-temperature superconductivity. *Nature* **396,** 733–735 (1998).
9. Hwang, J., Timusk, T. & Gu, G. D. High-transition-temperature superconductivity in the absence of the magnetic-resonance mode. *Nature* **427,** 714–717 (2004).
10. Tranquada, J. M. *et al.* Quantum magnetic excitations from stripes in copper oxide superconductors. *Nature* **429,** 534–538 (2004).
11. Axe, J. D. & Shirane, G. Influence of the superconducting energy gap on phonon linewidths in Nb_3Sn. *Phys. Rev. Lett.* **30,** 214–216 (1973).
12. Dai, P., Mook, H. A. & Dogan, F. Incommensurate magnetic fluctuations in $YBa_2Cu_3O_{6.6}$. *Phys. Rev. Lett.* **80,** 1738–1741 (1998).
13. Mook, H. A. *et al.* Spin fluctuations in $YBa_2Cu_3O_{6.6}$. *Nature* **395,** 580–582 (1998).
14. Arai, M. *et al.* Incommensurate spin dynamics of underdoped superconductor $YBa_2Cu_3O_{6.7}$. *Phys. Rev. Lett.* **83,** 608–611 (1999).
15. Bourges, P. *et al.* The spin excitation spectrum in superconducting $YBa_2Cu_3O_{6.85}$. *Science* **288,** 1234–1237 (2000).
16. Bourges, P. *et al.* High-energy spin excitations in $YBa_2Cu_3O_{6.5}$. *Phys. Rev. B* **56,** R11439–R11442 (1997).
17. Hayden, S. M. *et al.* Absolute measurements of the high-frequency magnetic dynamics in high-T_c superconductors. *Physica B* **241–243,** 765–772 (1998).
18. Fong, H. F. *et al.* Spin susceptibility in underdoped $YBa_2Cu_3O_{6+x}$. *Phys. Rev. B* **61,** 14773–14786 (2000).
19. Damascelli, A., Hussain, Z. & Shen, Z.-X. Angle-resolved photoemission studies of the cuprate superconductors. *Rev. Mod. Phys.* **75,** 473–541 (2003).
20. Timusk, T. & Statt, B. The pseudogap in high-temperature superconductors: an experimental survey. *Rep. Prog. Phys.* **62,** 61–122 (1999).
21. Christensen, N. B. *et al.* Universal dispersive excitations in the high-temperature superconductors. Preprint at ⟨http://arxiv.org/abs/cond-mat/0403439⟩ (2004).
22. Kivelson, S. A. *et al.* How to detect fluctuating stripes in the high-temperature superconductors. *Rev. Mod. Phys.* **75,** 1201–1241 (2003).
23. Shamoto, S., Sato, M., Tranquada, J. M., Sternlieb, B. & Shirane, G. Neutron-scattering study of antiferromagnetism in $YBa_2Cu_3O_{6.15}$. *Phys. Rev. B* **48,** 13817–13825 (1993).
24. Bulut, N., Hone, D., Scalapino, D. J. & Bickers, N. E. Random-phase approximation analysis of NMR and neutron-scattering experiments on layered cuprates. *Phys. Rev. Lett.* **64,** 2723–2726 (1990).
25. Norman, M. R. Relation of neutron incommensurability to electronic structure in high-temperature superconductors. *Phys. Rev. B* **61,** 14751–14758 (2000).
26. Hussey, N. E., Abdel-Jawad, M., Carrington, A., Mackenzie, A. P. & Balicas, L. A coherent three-dimensional Fermi surface in a high-transition-temperature superconductor. *Nature* **425,** 814–817 (2003).

Supplementary Information accompanies the paper on **www.nature.com/nature**.

Acknowledgements This work was supported in part by the UK EPSRC, the US NSF and the DOE.

Competing interests statement The authors declare that they have no competing financial interests.

Correspondence and requests for materials should be addressed to S.M.H. (S.Hayden@bristol.ac.uk).

Quantum magnetic excitations from stripes in copper oxide superconductors

J. M. Tranquada[1], H. Woo[1,2], T. G. Perring[2], H. Goka[3], G. D. Gu[1], G. Xu[1], M. Fujita[3] & K. Yamada[3]

[1] *Physics Department, Brookhaven National Laboratory, Upton, New York 11973, USA*
[2] *ISIS Facility, Rutherford Appleton Laboratory, Chilton, Didcot, Oxon OX11 0QX, UK*
[3] *Institute for Materials Research, Tohoku University, Sendai 980-8577, Japan*

In the copper oxide parent compounds of the high-transition-temperature superconductors[1] the valence electrons are localized—one per copper site—by strong intra-atomic Coulomb repulsion. A symptom of this localization is antiferromagnetism[2], where the spins of localized electrons alternate between up and down. Superconductivity appears when mobile 'holes' are doped into this insulating state, and it coexists with antiferromagnetic fluctuations[3]. In one approach to describing the coexistence, the holes are believed to self-organize into 'stripes' that alternate with antiferromagnetic (insulating) regions within copper oxide planes[4], which would necessitate an unconventional mechanism of superconductivity[5]. There is an apparent problem with this picture, however: measurements of magnetic excitations in superconducting $YBa_2Cu_3O_{6+x}$ near optimum doping[6] are incompatible with the naive expectations[7,8] for a material with stripes. Here we report neutron scattering measurements on stripe-ordered $La_{1.875}Ba_{0.125}CuO_4$. We show that the measured excitations are, surprisingly, quite similar to those in $YBa_2Cu_3O_{6+x}$ (refs 9, 10) (that is, the predicted spectrum of magnetic excitations[7,8] is wrong). We find instead that the observed spectrum can be understood within a stripe model by taking account of quantum excitations. Our results support the concept that stripe correlations are essential to high-transition-temperature superconductivity[11].

$La_{2-x}Ba_xCuO_4$ ('Zurich' oxide) is the material in which Bednorz and Müller[1] first discovered high-transition-temperature superconductivity. An anomalous suppression of the superconductivity found[12] in a very narrow region about $x = 1/8$ was later shown to be associated with charge and spin stripe order[4,13]. Schematic diagrams of stripe order in the CuO_2 planes are shown in Fig. 1a and b. Between the charge stripes are regions with locally antiferromagnetic order. The 'bond-centred' stripe model shown has received considerable theoretical attention[11,14–16].